On the application of the Stockwell transform to GPR data analysis

On the application of the Stockwell transform to GPR data analysis

Luigi Riba
Université de Pau et des Pays de l'Adour, LFC-R
Pau, France
luigi.riba@univ-pau.fr

Salvatore Piro
Institute of Technologies Applied to Cultural Heritage
ITABC-CNR
Montelibretti, Italy
salvatore.piro@itabc.cnr.it

Ubertino Battisti, Luigi Sambuelli
Politecnico di Torino - DISMA
Politecnico di Torino - DIATI
Torino, Italy
ubertino.battisti@polito.it
luigi.sambuelli@polito.it

***Abstract*—For most archaeological prospections with GPR, target detection is the most important aspect of the surveys. The main efforts of GPR data processing are committed to increase the signal to noise ratio in radargrams. The usual processing aims to: filter the radar section from clutters and attenuate the in-band noises; enhance coherent reflections that are likely due to the target response; transform the acquired time section into a depth section; build a 3D image of the reflection targets in the subsoil by correlating reflections from adjacent radargrams. In this paper we show some application of the Stockwell transform, both to synthetic and field data, to enhance the signal to noise ratio in radargrams.**

Keywords—GPR data; Stockwell transform; synthetic data; real data.

I. INTRODUCTION

For most archaeological prospections with GPR, target detection is the most important aspect of the surveys. Shallow and narrow features may require a very fine profiles density to get detected. The smallest detectable size of archaeological materials is also dependent on the wavelength of the signal transmitted by the antenna. A buried archaeological debris field, containing higher concentrations of small fragments of ancient habitation, e.g. flint chips or other materials, may show some scattered energies on the radargrams which may slightly differ with respect to areas where no debris are located. Unless a fortunate color transform is used, it is unlikely that these small reflections will ever be noticed within the radargram – vertical slice – dataset [1], [2]. Rather than showing the changes in reflected energies along the vertical - radargram - slices of the ground, it is often more useful to map horizontal changes of reflected energy across a site. In this case small but consistent reflections above the background noise can be visualized by using time slice analysis. Some of the main goals of GPR data processing are: to filter the radar section from clutters and attenuate in-band noises; to enhance coherent reflections likely due to the target response; to transform the acquired time section into a depth section; to build a 3D image of the reflection targets in the subsoil by correlating reflections from adjacent radargrams [1], [2]. In this paper we show some application of the Stockwell transform to synthetic data, produced with a finite difference code from a model, and field data from an archaeological survey, to enhance the signal to noise ratio in radargrams and time-slices.

II. THE STOCKWELL TRANSFORM

In many practical applications it is important to analyze signals, i.e . extracting the time/space and frequency content of the signal. Unfortunately, due to the Heisenberg uncertainty principle, it is impossible to simultaneously retain precise time and frequency information of a signal. Fourier transform provides all the frequency information (spectrum) of a signal but it cannot give any time/space information. Many techniques arose trying to deal with the uncertainty principle in order to obtain a "sufficiently good" time-frequency representation of a given signal. We recall here the short-time-Fourier transform, the Gabor transform and the wavelet transform.

The Stockwell Transform (S-transform) was first introduced in 1996 by R. G. Stockwell, L. Mansinha and R. P. Lowe [3] to deal with data coming from seismic digital analysis. The Stockwell transform can be seen as a mix between Short-Time Fourier Transform, sometimes called Gabor Transform, and the Wavelet Transform. Due to its flexibility, the Stockwell transform has been used for image filtering, texture recognition, noise reduction, image

compression and, in general, as a tool in image processing [4], [5], [6].

The precise expression of the S-transform of a signal f is the following:

$$S_f(b,\xi) = (2\pi)^{1/2}|\xi|\int e^{-2\pi i t\xi} f(t) e^{-\xi^2 (b-t)^2/2} dt$$

The parameter b represents the time localization of the signal, while the ξ parameter represents the frequency localization. Roughly speaking $S_f(b,\xi)$ represents the energy of the signal f at the time b and at the frequency ξ.The main idea is that the width of the analyzing window, usually a Gaussian, depends on the frequency. More precisely, as the frequency increases the width of the analyzing window shrinks. This property implies that the S-transform gains time localization as the frequency increases. That is, it is able to localize with high precision high frequencies of the signal.

The S-transforms shares some properties with the Wavelet transform [7]. The main difference is the meaning of the parameters involved. In the Wavelet case, the scale parameter a has not a real frequency meaning. In application it is used the relation

$$a^{-1} \propto \xi$$

which is essentially true only for small values of a and therefore large frequencies ξ. In the case of the S-transform the ξ parameter is really the frequency parameter. Moreover, the S-transform, in its phase, encompasses additional information. It has been proven that, at least for high frequencies, the phase of the S-transform gives a precise description of the instantaneous frequency of the signal [8], [9]. In this paper we do not exploit this feature, but it will be the next step in our analysis. These two remarks convinced us in analyzing the S-transform rather than the Wavelet transform.

In this paper we use a variant of the S-transform, called DOST (Discrete Orthonormal Stockwell Transform). The DOST of a signal of length N is a string of N coefficients, called DOST coefficients, which represent the energy of the signal in a certain time-frequency domain. That is, at a certain time and at a certain frequency. The DOST is much faster than the S-transform, it is as fast as the FFT, this fast algorithm was introduced by Y. Wang and J. Orchard [10]. Therefore, its application to images is possible and fruitful. The DOST parameters are not uniformly distributed in the time-frequency domain. More precisely, as far as the frequency increases we gain time (or spatial) localization and we lose frequency localization. In the paper we have used the 2-dimensional DOST written in Matlab which is available in www.mathworks.com [11]. (The algorithm has been written by U. Battisti and L. Riba, the complete url address is: http://www.mathworks.com/matlabcentral/fileexchange/ 47223-2-dimensional-dost-zip).

III. THE SYNTHETIC AND THE EXPERIMENTAL DATA

We applied the Stockwell transform to two data set: a synthetic one produced with a finite difference software (Reflexw©) starting from a subsurface model and the other one from archaeological GPR survey made on the Palatino hill in Rome (Italy).

A. *The model*

In order to test the effectiveness of the Stockwell transform we build, with the software Reflexw© a synthetic model consisting of a background soil (ε_r = 9, σ = 0.005 S/m, μ_r = 1) with three structures (ε_r = 4, σ = 0.001 S/m, μ_r = 1) having different shapes (Fig 1). We then added to the background a random noise in form of scattering objects with a volumetric density equal to 65%. The objects have sizes ranging from few centimeters up to 20 by 10 cm and their physical parameters have a white distribution around ε_r = 9 and σ = 0.005 S/m with variances equal to 2 and 0.004 S/m respectively.

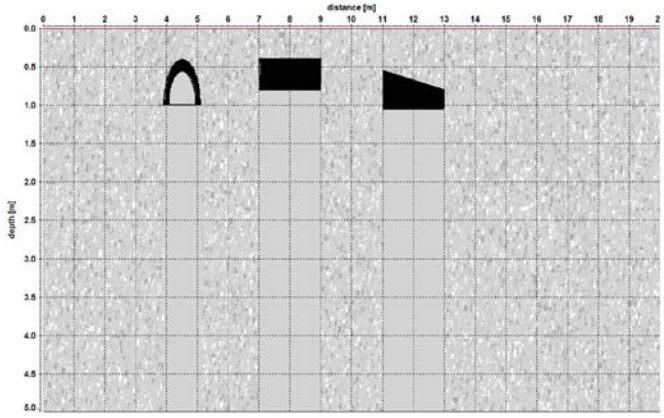

Fig. 1. Model of buried structures with white noise added on.

With the software Reflexw©, working with finite difference in time domain, we produced the synthetic radargram shown in the simulated acquisition parameters were: 0.01 m/scan, 0.03 ns as sampling interval, trace duration 30 ns and a central frequency of the antenna pulse equal to 200 MHz.

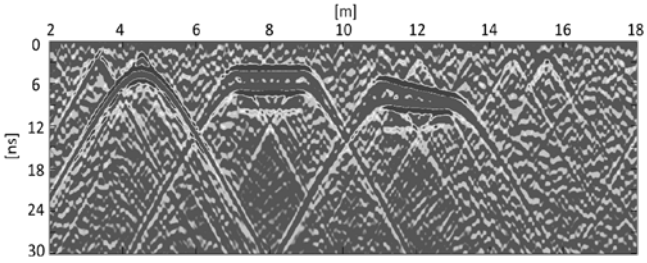

Fig. 2. Synthetic radargram obtained from the model in Fig.1.

B. *The archaeological site*

The study area is characterised by a sequence of complex buildings, related to the Roman period between the late Republican and Severo's age (200 AD). During the archaeological investigations made subsequent to the

geophysical surveys, from 2001 to 2004, between the N-E foot of Palatino Hill and the Colosseum Valley and nearest

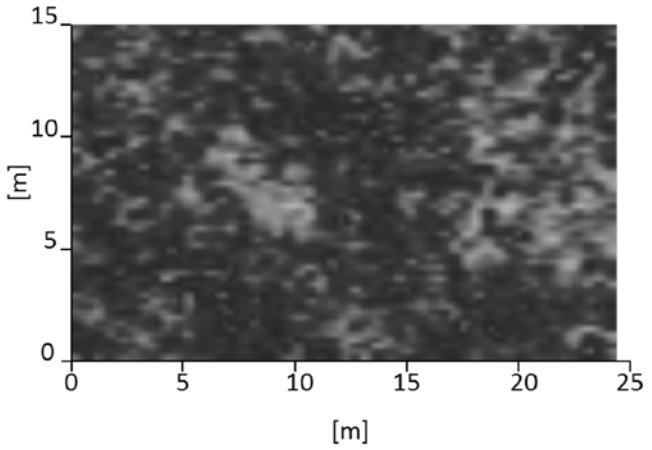

Fig. 3. Time slice n.13 from the Palatino hill survey after bandpass filtering and background removal.

Elagabalo's Thermae, a sequence of complex buildings, related to the Roman period between the late Republican and Severo's age were discovered. The oldest building is a *domus* of the late Republican period located in front of a line of buildings called *tabernae* which were used for shops and living quarters. This corridor of buildings connected the Colosseum Valley and the Roman Forum. The fire-raising of 64 A.C., signed the destruction of these buildings and the development of Neronian urbanism. The archaeological excavations have located a portion of the foundation of a portico, and a portion of a sewage system with S-N direction and a foundation with E shape, which defines and closes Elagabalo's Thermae.

On the Palatino hill we analyzed an area 24.5 by 15 square meters. We acquired, with a 500 MHz antenna and a GSSI Sir 10A+, 49 profiles each one with about 633 traces. The trace duration was 85 ns and the sampling frequency was 6 GHz. After background removal by subtracting the mean trace and bandpass filtering we made 45 time slices averaging 17 samples with an overlap equal to 5. In Fig 3 the absolute amplitude slice at about 1 m in depth is shown.

IV. Results and Discussion

If we would like to filter a given signal using the classical FFT we could take the signal, decompose it in a localized frequency basis via FFT, remove certain coefficients that satisfy a reasonable energy criterion and then reconstruct the signal using the IFFT.

The DOST filtering follows the same general approach but could allow us to have a finer description of the signal. In fact, via the DOST we decompose the given signal in a basis which is localized both in frequency and in space. So, we can remove certain coefficients without effecting the whole signal. This finer signal description allowed us to incorporate more a priori physical information in the filtering process. In fact, if, for example, we know that our signal cannot contain high frequency spikes in a certain area we could remove them locally. Clearly, it is impossible to define a general physical assumption that works with every kind of signal. In practice the knowledge of the problem has to orient the filter implementation. In studying GPR images we assumed the relevant portion of the image to be the most energetic. In other words, we assumed that the noise in the image has a lower energy content with respect to the signal. Notice that the DOST filtering can be used in a filtering pipeline. In our case, we first filtered the signal via DOST and then we applied a terracing. Both filtering steps are controlled by two parameters: (λ_1, λ_2). The first one controls the energy filtering and the second one controls the terracing level. After several numerical experiments we set these parameters equal to (15, 3) for the synthetic data and (3, 3) for the Palatino's data.

The filtering pipeline is composed of the following steps:

Step 1 We remove the main bang and the main horizontal reflections by computing the mean trace and then subtracting it from each trace.

Step 2 The 2-d DOST transform is applied to the radargram considered as an image, that is a 2-d matrix.

Step 3 We evaluate the mean μ and the standard deviation σ of the nonzero coefficients of the DOST transform of the radargram.

Step 4 We set to zero all DOST coefficients c_i such that

$$(c_1 - \mu) < \lambda_1 \cdot \sigma .$$

This means essentially that we want to consider coefficients with high energy which are sufficiently far from the mean. We are here supposing that the reflection event is rare, in the sense that they have energy much higher than the background.

Step 5 We finally apply a terracing. We evaluate again the mean value, μ', of the new DOST coefficients obtained in Step 4. And then we set to zero all coefficients c_i such that

$$(c_i) < \lambda_2 \cdot \mu' .$$

Step 6 Finally we perform the inverse DOST transform of the matrix obtained in Step 5.

The result of the filter is shown in Fig. 4. It is worthy to not how the filtering reduce the multiple reflections below the two structures at 8 and 12 m.

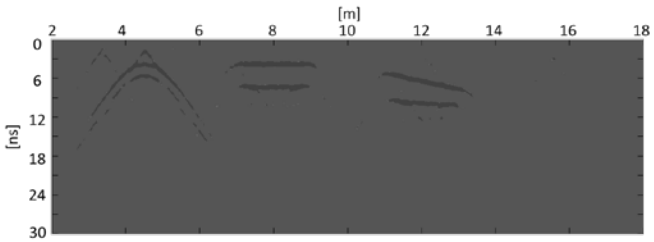

Fig. 4. Synthetic radargram from the model in Fig.1 after DOST filtering.

We analyze the data coming from the Palatino Hill using the filtering method described in Step 1 to Step 6.To have a clearer visualization of the filtered volume we perform the following additional steps:

Step 7 We remove the main bang and the main horizontal reflections by computing the mean trace and then subtracting it from each trace.

Step 8 The 2-d DOST transform is applied to the radargram considered as an image, that is a 2-d matrix.

The result of the filtering is shown in Fig. 5. In comparison with the same slice (Fig. 3) the DOST filtered slice has a reduced background noise and delineates some structures in the lower left part of the investigated area.

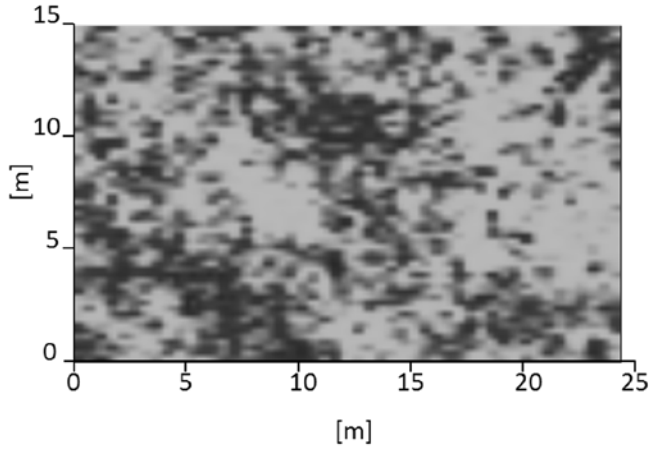

Fig. 5. Time slice n.13 from the Palatino hill survey after background removal and DOST filtering.

V. CONCLUSIONS

The Stockwell transform, whenever the energy content of signal and noise are identifiable and different, seems to be able to filter the radargrams with a noticeable precision. Its local properties allow for a selective cleaning and an overall increasing of the signal to noise ratio useful for enhancing the further time slice and 3D rendering processing.

VI. ACKNOWLEDGMENT

The Authors would like to thank Daniela Zamuner (ITABC) for help in Palatino data acquisition.

VII. REFERENCES

[1] D. Goodman, and S. Piro, 2013. GPR Remote sensing in Archaeology. Springer. ISBN 978-3-642-31856-6, ISBN 978-3-642-31857-3 (eBook), DOI 10.1007/978-3-642-31857-3.

[2] S. Piro, 2006. Indagini Georadar ad alta risoluzione nell'area delle pendici nord-orientali del Palatino. In *Scienze dell'Antichità, Storia, Archeologia, Antropologia*, Edizioni Quasar, 13, pp.141-156

[3] R. G. Stockwell, L. Mansinha, and R. P. Lowe., 1996. Localization of the complex spectrum: the S-transform., IEEE Transactions on Signal Processing , 44, pp. 998-1001.

[4] S. Azadi, and A. A. Safavi, 2011. S-Transform Based P-wave and S-wave Arrival Times Measurements Toward Earthquake Locating. 2nd International Conference on Control, Instrumentation and Automation (ICCIA).

[5] N. E. Zabihi, and H.R. Siahkoohi, 2006. Single Frequency Seismic Attribute Based on Short Time Fourier Transform, Continuous Wavelet Transform, and S Transform. 6th International Conference and Exposition on Petroleum Geophysics.

[6] R.S. Choraś, 2014. Time–Frequency Analysis of Image Based on Stockwell Transform. in: Image Processing and Communications Challenges 5, in: Advances in Intelligent Systems and Computing, vol.233, Springer International Publishing, pp.91–97.

[7] L. Riba, 2014. Multi-dimensional Stockwell Transforms and Applications. PhD thesis, Università degli Studi di Torino, Italy, available at https://aperto.unito.it/handle/2318/142144?mode=full#.VWcJ_aFIxWV.

[8] Q. Guo, S. Molahajloo, and M. W. Wong, 2010. Phases of Modified Stockwell Transforms and Instantaneous Frequencies. Journal of Mathematical Physics. 51, pp. 052101–1 – 052101–11.

[9] E. Sejdic , L. Stankovic, M. Dakovic, and J. Jiang, 2008, Instantaneous Frequency Estimation using the S-Transform. IEEE signal processing letters.

[10] Y. Wang and J. Orchard , 2009. Fast discrete orthonormal Stockwell transform. SISC , 31, pp. 4000-4012.

[11] U. Battisti, and L. Riba, 2015. Window-dependent bases for efficient representations of the Stockwell transform. in press on ACHA.

.